Final Draft
of the original manuscript:

Srinivasan, B.; Liang, J.; Blawert, C.; Stoermer, M.; Dietzel, W.:
Characterization of calcium containing plasma electrolytic oxidation coatings on AM50 magnesium alloy
In: Applied Surface Science (2010) Elsevier

DOI: 10.1016/j.apsusc.2010.01.069

Characterization of calcium containing plasma electrolytic oxidation coatings on AM50 magnesium alloy

P. Bala Srinivasan*, J. Liang, C. Blawert, M. Störmer, W. Dietzel
Institute of Materials Research
GKSS-Forschungszentrum Geesthacht GmbH
D-21502 Geesthacht, Germany

*Corresponding Author (bala.srinivasan@gkss.de);
Phone: 00-49-4152-871997; Fax: 00-49-4152-871960

Keywords
Magnesium alloy; plasma electrolytic oxidation; microstructure; corrosion behaviour.

Abstract

An attempt was made to produce calcium containing plasma electrolytic oxidation (PEO) coatings on AM50 magnesium alloy using an alkaline electrolyte. This study was performed in three alkaline electrolytes containing calcium hydroxide and sodium phosphate with three different mass ratios viz., 1:2.5, 1:5 and 1:7.5. All the three coatings produced were found to contain Ca and P in appreciable amounts. The concentration of P was found to be higher in the coatings obtained in the electrolytes with higher concentration of phosphate ions. Even though all the three coatings were found to be constituted with magnesium oxide and magnesium phosphate phases, X-ray diffraction analyses revealed that the phase composition was influenced by the phosphate ion concentration/conductivity of the electrolyte. Further, the PEO coating obtained in the 1:7.5 ratio electrolyte was found to contain di-calcium phosphate (monetite) and calcium peroxide phases, which were absent in the other two coatings. Potentiodynamic polarization studies performed in 0.1 M NaCl solution showed that the coatings obtained from the 1:5 ratio electrolyte possessed a superior corrosion resistance, which is attributed to the combined effect of thickness, compactness and phase/chemical composition of this coating.

Introduction

Light weight magnesium alloys possess good mechanical properties and excellent damping capabilities [1] and their strength-to-weight ratio makes them attractive for automotive applications [2]. However, their inherent poor corrosion resistance is a serious drawback for their usage in corrosive environments [3-4]. Among a variety of surface treatments contemplated for the corrosion protection of magnesium alloys [5-8], the plasma electrolytic oxidation (PEO) has became very popular since the beginning of this century [9-13]. These PEO coatings obtained from a spectrum of electrolytes offer a much superior corrosion and wear resistance compared to most of the other coatings produced by conventional low-voltage anodizing, , electroplating, vapour deposition etc.

In recent times, magnesium alloys are being considered as candidate materials for bio-medical applications owing to their bio-degradable nature [14-15]. These alloys can be used in such applications with or without additional surface treatments. By surface treatments a better control of the degradation rate of these alloys is intended when used as implant material, and also to facilitate the growth of tissues. Recent publications highlighted the applicability of hydroxyapatite coatings by a simple immersion treatment [16] and electro-deposition [17]. Yao et al [18] studied the feasibility of obtaining a silicate based PEO coating containing calcium and demonstrated the possibility of adjusting the Ca/P ratio in the coating. This investigation is an attempt to develop coatings on a magnesium alloy by PEO processing using electrolytes that contain calcium ions and to assess the coating formation, microstructural features, phase/chemical composition and corrosion behaviour.

Experimental

An AM50 magnesium alloy with a nominal composition of (mass fraction) 4.4 to 5.5% Al, 0.26 to 0.6% Mn, max 0.22% Zn, max 0.1% Si, and balance Mg was used in this investigation. Specimens of size 15 x 15 x 5 mm were polished using 320, 500 and 1500 grit emery sheets successively and cleaned with ethanol before the PEO treatment.

The PEO treatment was carried out using a unipolar pulsed power source in alkaline phosphate electrolytic solutions. During the PEO process, the magnesium alloy sample and the wall of the stainless steel container were used as the anode and cathode, respectively. The PEO electrolytes were constituted with calcium hydroxide and sodium

phosphate with three different mass ratios viz., 1:2.5 (2 g/L $Ca(OH)_2$ + 5 g/L Na_3PO_4), 1:5 (2 g/L $Ca(OH)_2$ + 10 g/L Na_3PO_4), and 1:7.5 (2 g/L $Ca(OH)_2$ + 15 g/L Na_3PO_4), respectively. The conductivity of the electrolytes was measured using a Mettler Toledo Inlab730 probe. The coatings were produced at an optimized constant current density of 30 $mA \cdot cm^{-2}$, with pulse on-off durations of 2 ms and 18 ms, respectively. The treatment duration was 15 minutes in all the cases. The temperature of the PEO electrolytes was kept at 20 ± 2˚C with the use of a cooling system. For ease of referencing, the coatings obtained in the 1:2.5, 1:5 and 1:7.5 ratio electrolytes are referred to as A, B and C, respectively, in the discussions.

The surface roughness of the coatings was assessed using a Hommel profilometer. Coating thickness measurements were made with a Minitest 2100 non-destructive thickness meter. X-ray diffraction (XRD) was performed using a Bruker diffractometer with Cu-Kα radiation to determine the phase composition of the PEO coatings. Scanning electron microscopy (SEM) was used to examine the surface morphology and cross-section of the PEO coatings. The elemental composition of the coatings was assessed in a Zeiss Ultra55 SEM equipped with an energy dispersive spectrometer (EDS).

The corrosion behaviour of the PEO coated magnesium alloy specimens was assessed by potentiodynamic polarisation tests which were carried out using ACM Gill AC computer controlled potentiostat. A typical three electrode cell with the coated specimen as the working electrode (0.5 cm^2 exposed area), a saturated Ag/AgCl electrode as the reference electrode, and a platinum mesh as counter electrode was used. The tests were performed at a scan rate of 0.5 mV/s after an exposure period of 30 minutes.

Results and Discussion

Voltage vs. time behaviour

The voltage vs. time plots obtained during the PEO processing of AM50 magnesium alloy substrates in the three electrolytes are shown in **Figure 1**. The PEO processing of magnesium alloys is characterized by four different stages viz., (i) initial dissolution/passive film formation, (ii) breakdown of passive film and evolution of fine discharges, (iii) transitory phase involving changes in shape, size, density and colour of moving sparks and (iv) the stage of long-lived large-sized sparks of reduced density. As can be seen from Figure 1, the dissolution-film formation stage in electrolyte A was

observed up to around 255 V where the breakdown of film and evolution of fine discharges were noticed on the specimen surface. The second and third stages were found to pass through quickly in this electrolyte, reaching 465 V in less than 3 minutes. Thereafter, the increase in voltage was slowed down drastically, and a final voltage of 500 V was registered at the end of 15 minutes of treatment. In the electrolyte B, the sparking occurred a little bit earlier than in electrolyte A. Even though it was not possible to observe the density and intensity of sparks due to the turbidity of this electrolyte B, a slightly sluggish rate of increase in voltage could be noticed. Based on the change in slope, the second, third and fourth stages have been defined in the plot. The voltage reached a value of 450 V in 5 minutes and the plateau over the next 10 minutes of treatment took it to a final value of 485 V. In electrolyte C also, the breakdown was noticed at a much lower voltage compared to electrolyte B. Similar to the earlier case, this electrolyte was also too turbid to observe the spark characteristics, and hence the different stages could only be defined based on the voltage raise. Even though the first and second stages in electrolyte C appear to be closer to those observed in electrolyte B, the third stage was completely different. The voltage raise was found to be extremely slow, and it reached a value of around 420 V after about 12 minutes. A little ramp in the voltage seen after 12 minutes could be considered as the beginning of the fourth stage.

The distinct deviations in the above observed behaviour is attributed to the differences in the conductivity of the three electrolytes. The conductivities of the electrolytes A and B were 23.5 and 28.5 $mS.cm^{-1}$, respectively, as against a value of 37.3 $mS.cm^{-1}$ of electrolyte C. It is well known that the breakdown voltage during PEO processing decreases with an increase in conductivity of electrolyte **[19]** and hence it is not surprising that the higher conductivity electrolyte C had exhibited a lower breakdown voltage. While the increase in voltage during the PEO process up to the point of breakdown is predominantly governed by the electrolyte conductivity, the subsequent increase is influenced by the combined effect of electrolyte conductivity and thickness of the film/coating formed on the surface as the voltage is a function of applied current and the resistance offered at the solution/surface interface to the flow of current.

Microstructure

Scanning electron micrographs of the PEO coating A showing the surface morphology and the cross-section are shown in **Figures 2a and 2b**, respectively. The surface had numerous pores of different sizes in the range 1 μm to 15 μm. Most of the pores were

spherical; however, some irregularly shaped and lenticular pores were also observed. While many of these surface pores were apparently open, some of them appeared to have been filled with some compounds. The mean surface roughness (R_a) of the coating was found to be 1.4±0.1 μm. Thickness measurements using the eddy current probe showed values in the range of 18 μm to 23 μm, assessed in about 20 different locations over the surface area (15 x 15 mm²) of multiple specimens. The cross-section of the coating A, shown in Figure 2b reveals that the coating was fairly compact, with a few isolated fine pores and with some pores filled with compounds as well. The SEM micrograph shows a thickness of around 20 μm, which corroborate the data obtained from the thickness probe.

The surface and cross-sectional morphology of the PEO coating obtained from electrolyte B were different from A, as can be seen in **Figures 3a and 3b**. Even though the pore morphology was similar to that in the coating A, the pore density of this coating seemed to be much lower than that observed in the other case. The coating compounds appeared to have been deposited as relatively large chunks, and closed many open pores. Nevertheless, this surface was found to contain a good number of fine pores distributed uniformly. This coating had a higher surface roughness (2.8±0.3 μm) compared to that of coating A, which is also apparent from the protrusion-like surface regions seen in the micrograph (Figure 3a). The thickness of the coating B as measured by the eddy current probe was between 35 μm and 44 μm in different locations, and the SEM micrograph presented in Figure 3b substantiates this observation. In the cross-section, this coating was compact and similar features as those of the coating obtained from electrolyte A were observed.

In the case of coating C also the surface contained relatively large chunks of deposits with a few larger sized pores, as can be observed in **Figure 4a**. The coating thickness was in the range from 57 μm to 69 μm, based on the assessment over 20 locations on multiple specimens. The surface roughness of this coating was 4.5±0.3 μm. The cross-section of the specimen shown in **Figure 4b** reveals a number of large sized pores filled with compounds and also the presence of hairline micro-cracks.

In order to relate the conductivity of the electrolyte, coating thickness and the processing voltage, experiments were interrupted at 5 minutes and 10 minutes in all the three cases. The average thickness of coatings obtained in the aforementioned durations (5 minutes and 10 minutes, respectively) in the electrolytes A, B and C were

as follows: A: 10 μm and 14 μm; B: 20 μm and 30 μm; C: 36 μm and 55 μm. A closer look at the voltage vs. time plots suggests that the electrolyte conductivity had a greater influence not only on the voltages realized, but also on the thickness of the coatings. The higher conductivity of the electrolyte seemed to have facilitated a higher degree of plasma-chemical reactions, leading to the formation of a thicker coating. Ding et al **[20]** reported a similar effect of conductivity of electrolytes during the PEO processing in silicate electrolytes containing different concentrations of sodium tungstate. However, they did not mention how conductivity of the electrolytes affected the thickness of coatings. Considering the size of pores, the energy of discharges seemed to be higher in electrolyte C. As the voltage was lower, the peak current at the beginning of each pulse was apparently much higher, which is due to the higher conductivity of the electrolyte; and as the total current density was the same, the number of discharges was lower in case C. This is consistent with the microstructural observation that the coating C had a smaller number of pores compared to A.

Chemical and phase composition

Energy dispersive spectra of the coatings A, B and C are presented in **Figures 5a, b and c**, respectively. Mg, O, P, Ca and Na were the major elements identified in the coatings, in addition to traces of Al. The oxygen content in all the coatings was nearly the same. The magnesium concentration was higher by about 10% in coating A compared to that in the other two coatings. Na and P contents were found to increase with increase in sodium phosphate in the processing electrolytes. The calcium content was nearly the same in the coatings A and B; however, in the higher phosphate containing coating, the Ca concentration was lower the reason for which is not understood at this moment.

The coating A was found to be constituted predominantly with magnesium oxide (MgO), as evidenced from the XRD pattern in **Figure 6**. In addition, there was only a small peak corresponding to magnesium phosphate, $Mg_3(PO_4)_2$ phase. Earlier publications on the PEO of magnesium alloys in phosphate based electrolytes containing potassium hydroxide reported that the coatings were constituted either only with MgO or with substantial amounts of ($Mg_3(PO_4)_2$) phase, as well. **[21-22]**. However, given the fact that in this work the electrolyte was constituted with calcium hydroxide and sodium phosphate, and that the EDS analysis showed appreciable calcium content, it is surprising that no calcium containing compounds could be identified by XRD in this coating A. Yao et al., in their work on adjustment of the ratio of Ca/P in the ceramic

coating on magnesium alloy by plasma electrolytic oxidation also reported a similar result. i.e. that the XRD analysis did not show any calcium containing compounds in the coating, whilst the EDS analysis revealed appreciable amounts of calcium **[18]**.

In coating B, obtained in a higher phosphate concentration electrolyte, a high number of $Mg_3(PO_4)_2$ peaks were noticed in addition to the MgO phase. Further, the XRD spectrum in the 2θ range of 20° - 35° was like a mound, indicating the possibility of presence of some phases in amorphous form. The increased P concentration observed in the EDS analysis supplement the presence of magnesium phosphate phase in the coating. However, as like in the coating A, no peaks corresponding to calcium containing compounds could be identified in this coating, despite the revelation of high at.% of calcium in the EDS analysis. It is probable that calcium containing compounds could have been present in amorphous form in this coating. In the XRD spectrum of coating C, peaks corresponding to the calcium containing compounds viz., di-calcium hydrogen phosphate (monetite-$CaH(PO_4)_2$) and calcium peroxide (CaO_2), were seen in addition to the MgO and $Mg_3(PO_4)_2$ phases. Numerous peaks corresponding to these compounds were observed in the 2θ range of 20° - 40°, which coincided with the amorphous mound noticed in the XRD pattern of coating B.

The evolution of new compounds in the coatings in the higher phosphate concentration electrolytes can mainly be attributed to their conductivity. The higher conductivity was found to influence the peak current in individual pulses, giving a higher energy per pulse, and thus facilitating a rapid coating growth. In addition, the higher energy per pulse was also believed to be responsible for the enhanced plasma-chemical reactions in promoting the crystallization of the new phases/compounds. Hence, the coatings produced in the B and C electrolytes had significant differences in the chemical and phase composition.

Electrochemical corrosion behaviour

The electrochemical corrosion behaviour of the coatings obtained in the three electrolytes was assessed by potentiodynamic polarisation technique in neutral 0.1 M NaCl solution. The free corrosion potential and the corrosion current density for the uncoated AM50 magnesium alloy substrate were -1452 mV vs. Ag/AgCl and 1.8×10^{-2} $mA \cdot cm^{-2}$, respectively. The free corrosion potential of coating A was found to be in the active direction to that of the untreated alloy, registering a value of -1520 mV vs. Ag/AgCl. The corrosion potential of AM50 magnesium alloy with a silicate based PEO

coating was found to be slightly nobler than the magnesium substrate and that with a phosphate based PEO coating was in the active direction [23]. It appears that the presence of Mg_2SiO_4, the predominant phase in the silicate based PEO coating controlled the corrosion potential to drift towards the nobler side. On the other hand, the MgO and $Mg_3(PO_4)_2$ phases seemed to have governed the potential in the phosphate based PEO coating, and pushed it towards the active side. In this work, too, the coating A was constituted predominantly with MgO and small amounts of $Mg_3(PO_4)_2$, and hence the drift in corrosion potential towards the active side was in line with the earlier observation for a coating with a similar phase composition. Interestingly, the corrosion potentials of the other two coatings were found to drift slightly towards the nobler side than the coating A, with values of -1505 mV and -1495 mV vs. Ag/AgCl, respectively, which can be attributed to the presence of calcium containing phases in the coating. Nevertheless, the differences in the coating thickness and phase composition do not seem to influence the corrosion potential of the coated substrates much. However, the effects of the aforementioned factors on the corrosion current density and on the breakdown potentials can be seen in **Figure 7**. The corrosion current density values of the coatings A, B and C were 2.3 x 10^{-4} mA·cm^{-2}, 3.5 x 10^{-5} mA·cm^{-2}, 5.2 x 10^{-5} mA·cm^{-2}, respectively, and the breakdown potentials were -1475 mV, -1420 mV and -1390 mV vs. Ag/AgCl, respectively. Even though the coating C was having a higher thickness and also contained additional phases, this coating showed a slightly lower general corrosion resistance which is possibly on account of the microstructural features. Coating A was relatively thin and hence it should be expected that its corrosion behaviour is inferior to that of coating B. But, one would expect the coating C, with a higher thickness and additional phases to have exhibited a better general corrosion resistance than coating B. As was discussed in the earlier section, the coating C had numerous micro cracks in the cross-section, and this had apparently permeated the corrosive electrolyte to the substrate, thus resulting in a relatively higher corrosion current density than coating B. However, this coating still had exhibited a higher resistance to localized damage, as evidenced by the higher breakdown potential value. The polarisation studies suggest that the corrosion performance of the three PEO coatings was governed synergistically by the thickness, compactness and phase composition of the coatings.

From this investigation it was understood that it is possible to obtain a compact, thick, calcium containing PEO coating on magnesium alloys from calcium containing electrolytes. The long term corrosion behaviour of these calcium containing coatings is still to be assessed. Xu et al. [24] have recently demonstrated that Ca-P coatings

containing $CaH(PO_4)_2$ provided the magnesium alloy with a significantly better surface cytocompatibility and an improved osteoconductivity. It is planned to extend the PEO treatment and the subsequent investigations on potential bio-degradable alloys for possible applications as bio-implants.

Conclusions

Plasma electrolytic oxidation of AM50 magnesium alloy in a calcium hydroxide based electrolyte containing varying concentrations of sodium phosphate can yield coatings of different thickness levels under similar processing conditions. The changes in the discharge energy influenced by the conductivity of the electrolyte and the associated plasma-chemical reactions were found to be responsible for the different morphological features, surface roughness, phase composition and corrosion behaviour of the coatings. Coatings produced in a high conductivity electrolyte C (1:7.5 ratio electrolyte) contained calcium containing compounds viz., di-calcium hydrogen phosphate and calcium peroxide. The corrosion behaviour was influenced by the combined effect of thickness, compactness and phase/chemical composition of the coating. The calcium containing coatings can be a potential candidate for applications on bio-degradable magnesium alloys for bio-medical applications.

Acknowledgments

P. Bala Srinivasan and J. Liang express their sincere thanks to the Hermann-von-Helmholtz Association, Germany, and DAAD, Germany, for the award of fellowship and funding. The technical support of Mr. V. Heitmann, Mr. U. Burmester and Mr. V. Kree during the course of this work is gratefully acknowledged.

References

1. B.L. Mordike, T. Ebert, Materials Science and Engineering, A302 (2001) 37.
2. H. Westengen, Light Metal Age, 58 (2000) 44.
3. G. Song, A. Atrens, Advanced Engineering Materials, 1 (1999) 11.
4. E. Ghali : Magnesium and Magnesium alloys, in Uhlig's Corrosion Handbook, R.W. Revie, ed., John Wiley, New York, 2000, Ch. 44, pp. 793–830.
5. K. Brunelli, M. Dabala, I. Calliari, M. Magrini, *Corrosion Science,* 47 (2005) 989.

6. C. Blawert, V. Heitman, W. Dietzel, M. Stoermer, Y. Bohne, S. Maendl, B. Rauschenbach, Materials Science Forum, 539-543 (2007) 1679.

7. A. Bakkar, V. Neubert, Electrochemistry Communications, 9 (2007) 2429

8. J.E. Gray, B. Luan, Journal of Alloys and Compounds, 336 (2002) 88.

9. C. Blawert, W. Dietzel, E. Ghali, G. Song, Advanced Engineering Materials, 8 (2006) 511.

10. H. Guo, M. An, S. Xu, H. Huo, Materials Letters, 60 (2006) 1538

11. P. Bala Srinivasan, J. Liang, C. Blawert, M. Störmer, W. Dietzel, Applied Surface Science, 255 (2009) 4212.

12. H. Duan, C. Yan, F. Wang, Electrochimica Acta, 52 (2007) 3785.

13. J. Liang, T. Hu, J. Hao, Electrochimica Acta, 52 (2007) 4836.

14. M.P. Staiger, A.M. Pietak, J. Huadmai, G. Dias, Biomaterials 27 (2006) 1728.

15. F. Witte, F. Feyerabend, P. Maier, J. Fischer, M. Störmer, C. Blawert, W. Dietzel, N. Hort, Biomaterials, 28 (2007) 2163.

16. C. Wen, S. Guan, L. Peng, C. Ren, X. Wang, Z. Hu, Applied Surface Science, 255 (2009) 6433.

17. Y.W. Song, D.Y. Shan, E.H. Han, Materials Letters, 62 (2008) 3276.

18. Z.Yao, L. Li, Z. Jiang, Applied Surface Science, 255 (2009) 6724.

19. S. Ikonopisov, Electrochimica Acta, 22 (1977) 1077.

20. J. Ding, J. Liang, L. Hu, J. Hao, Q. Xue, Transactions of Non-Ferrous Metals Society of China, 17 (2007) 244.

21. J. Liang, L. Hu, J. Hao, Applied Surface Science, 253 (2007) 4490.

22. R. Arrabal, E. Matykina, F. Viejo, P. Skeldon, G.E. Thompson, Corrosion Science, 50 (2008) 1744.

23. J. Liang, P. Bala Srinivasan, C. Blawert, M. Stöermer, W. Dietzel, Electrochimica Acta, 54 (2009) 3842.

24. L. Xu, F. Pan, G. Yu, L. Yang, E. Zhang, K. Yang, Biomaterials, 30 (2009) 1512.

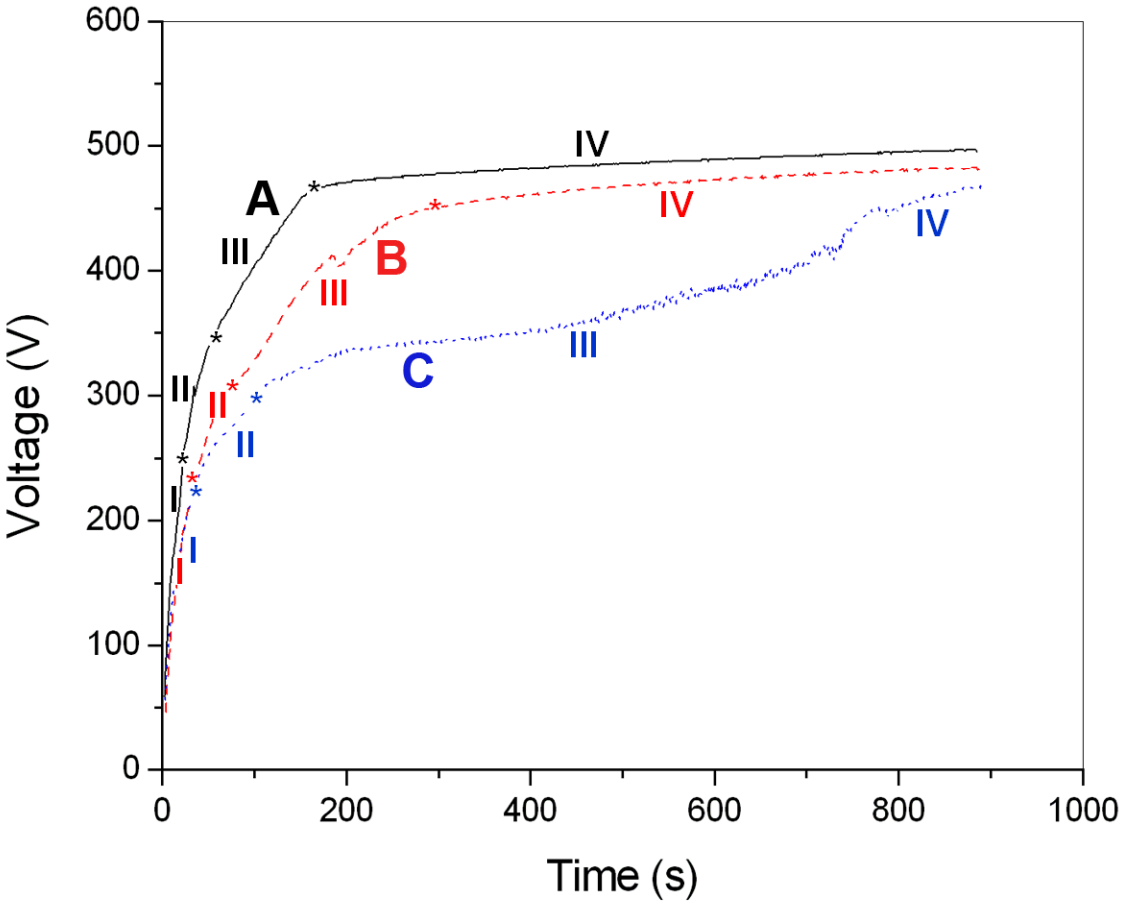

Figure 1 Voltage vs. time plots obtained during the evolution of coating in three different electrolytes

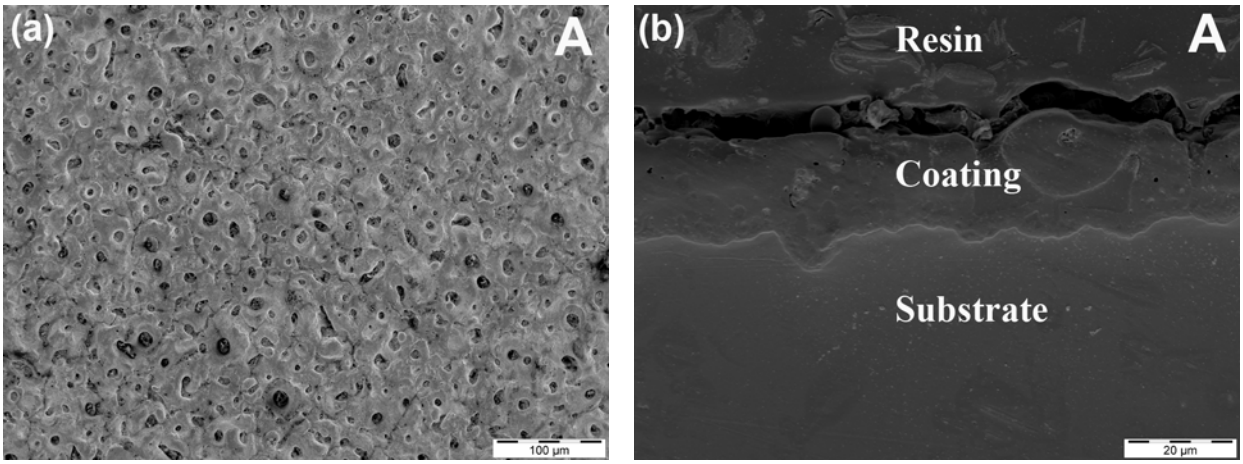

Figure 2 Scanning electron micrographs showing the (a) surface morphology and (b) cross-section of the PEO coating “A”.

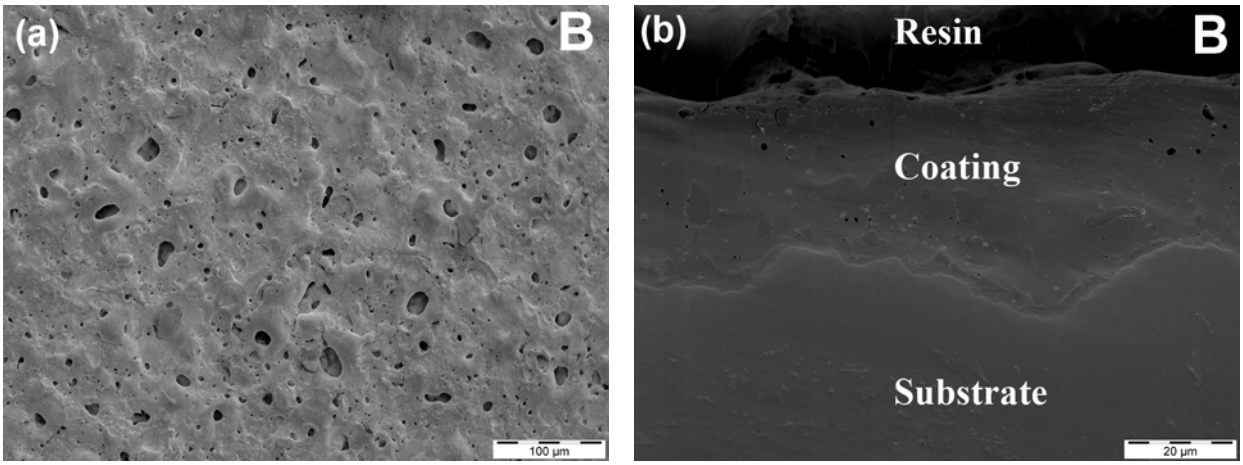

Figure 3 Scanning electron micrographs showing the (a) surface morphology and (b) cross-section of the PEO coating “B”.

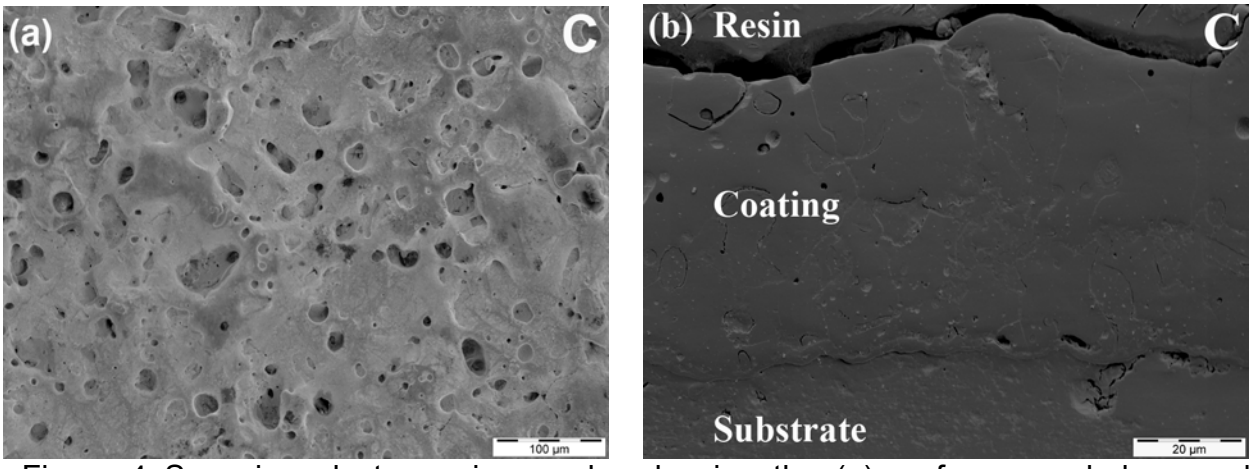

Figure 4 Scanning electron micrographs showing the (a) surface morphology and (b) cross-section of the PEO coating “C”.

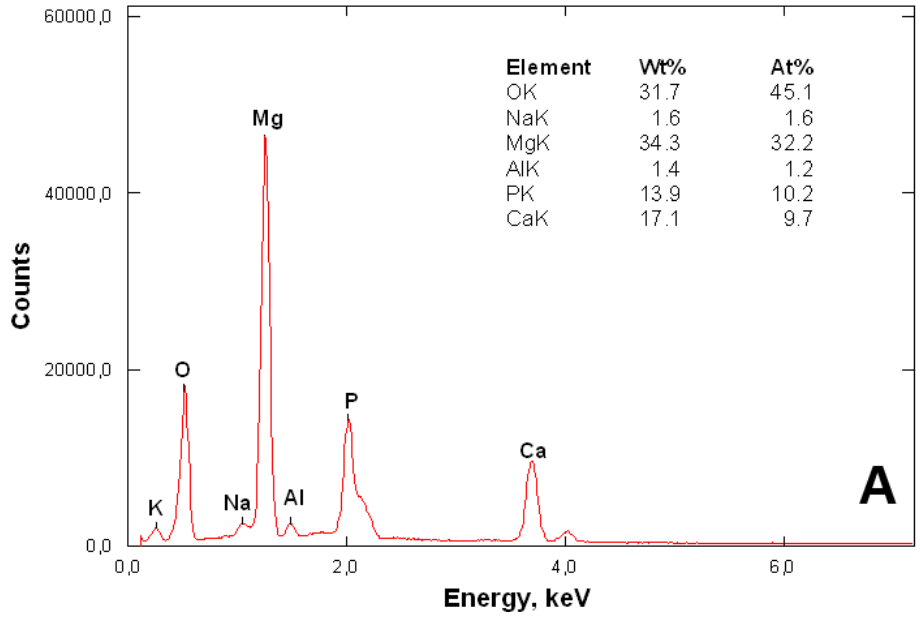

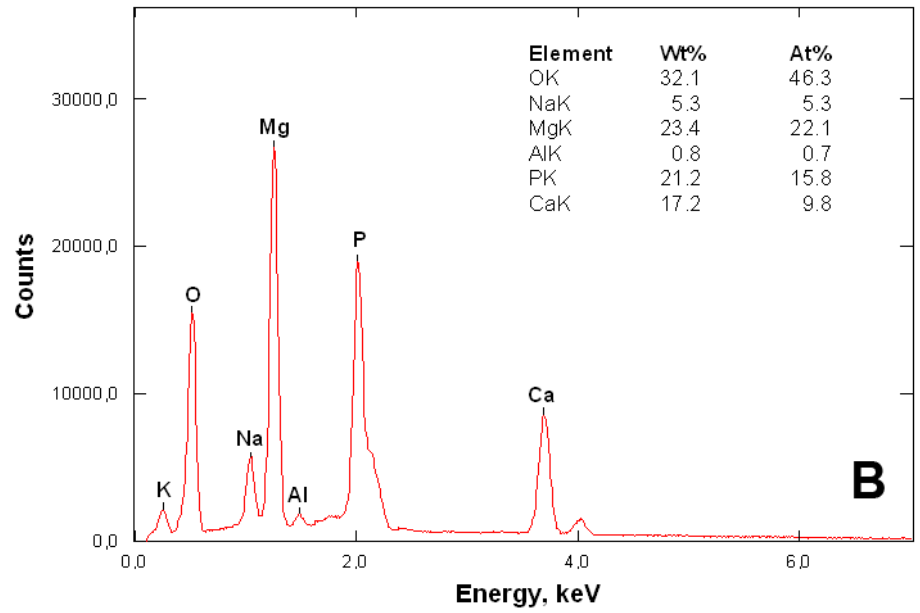

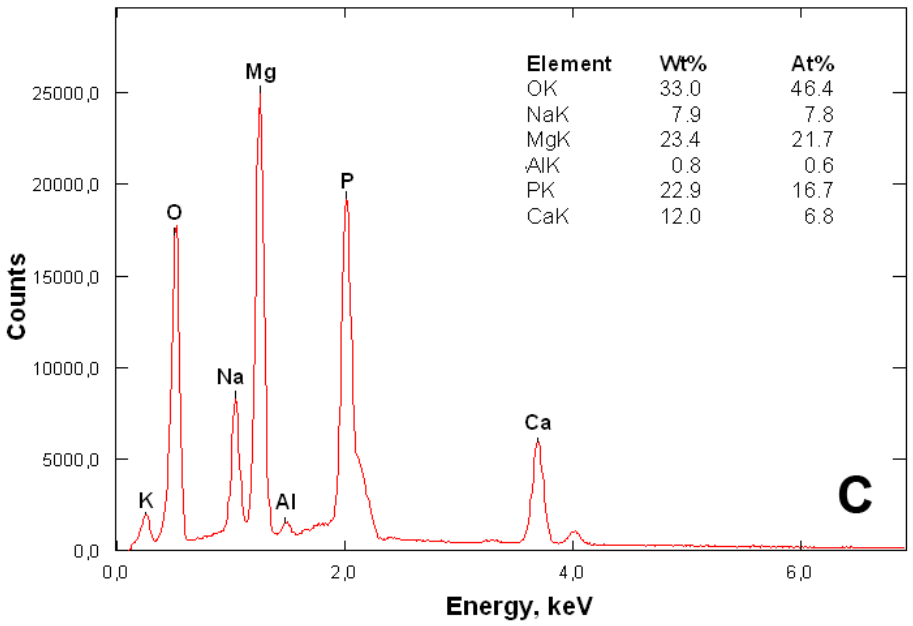

Figure 5 Energy dispersive spectra of the different PEO coated AM50 alloy specimens.

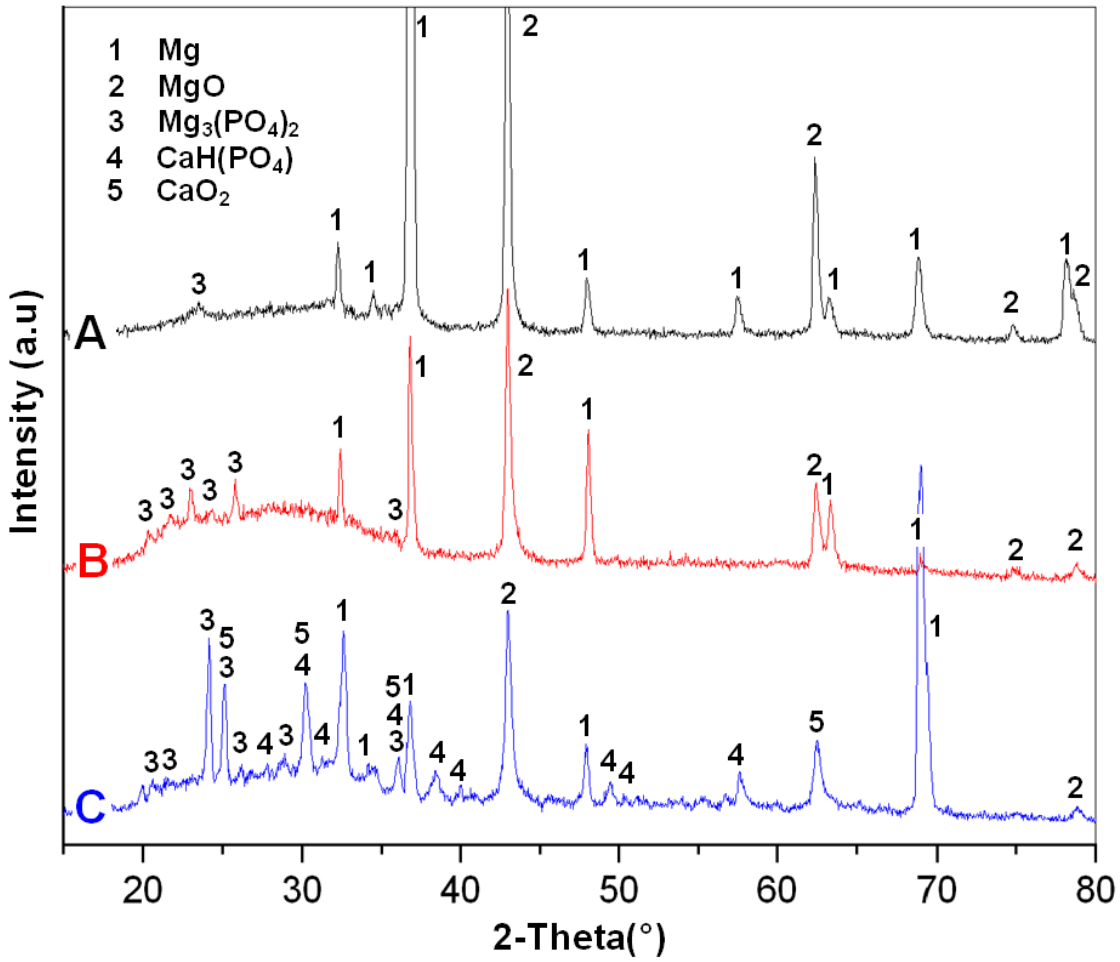

Figure 6 X-Ray diffraction patterns of the three different PEO coated AM50 alloy specimens.

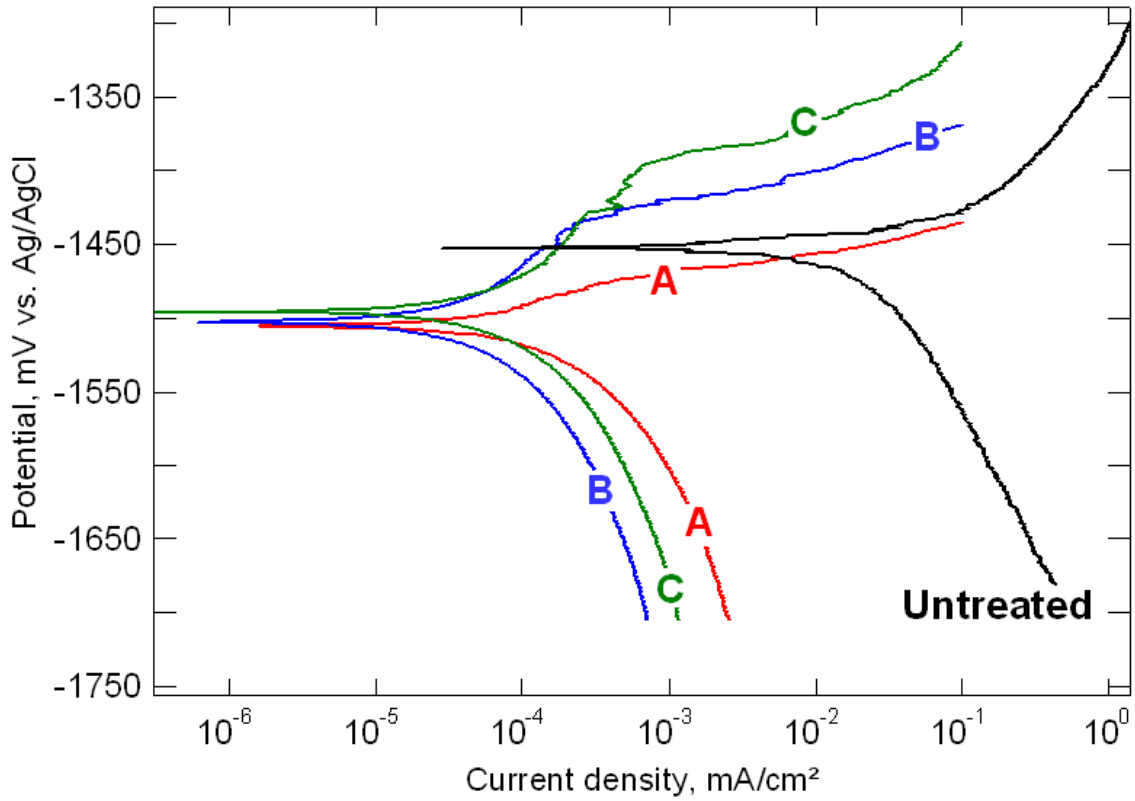

Figure 7 Potentiodynamic polarization behaviour of the PEO coated AM50 alloy specimens (Test solution: 0.1M NaCl).